A Numerical Study on the Smoke Behavior by Solar Radiation through Ceiling Glass in Atrium Fires

Jin-Yong Jeong*

Key words: Smoke filling process, Heat flux, SMEP, Atrium, Field model, Zone model

Abstract

This paper describes the smoke filling process of a fire field model based on a self-developed SMEP (Smoke Movement Estimating Program) code to the simulation of fire induced flows in the two types of atrium space containing a ceiling heat flux. The SMEP using PISO algorithm solves conservation equations for mass, momentum, energy and species, together with those for the modified $k-\varepsilon$ turbulence model with buoyancy production term. Also it solves the radiation equation using the discrete ordinates method. Compressibility is assumed and the perfect gas law is used. Comparison of the calculated upper-layer average temperature and smoke layer clear height with the zone models has shown reasonable agreement. The zone models used are the CFAST and the NBTC one-room. For atrium fires with ceiling glass the ceiling heat flux by solar heat causes a high smoke temperature near the ceiling. However, it has no effect on the smoke movement such as the smoke layer clear heights that are important in fire safety. In conclusion, the smoke layer clear heights that are important in evacuation activity except the early of a fire were not as sensitive as the smoke layer temperature to the nature of ceiling heat flux condition. Thus, a fire sensor in atrium with ceiling glass has to consider these phenomena.

Nomenclature

A : fire source area [m^2]
$a_{\varepsilon,i}$: emissivity weighting factors for the i-th gray gas
C_P : specific heat of plume gases [kJ/kgK]
D_f : diameter of fire [m]
I_w : wall radiation intensities [W/(m^2 · sr)]
$\dot{m}$: mass flow rate [kg/s]
Q : heat release rate of the fire [kW]
Q_C : convective of the heat release rate [kW]
T_w : wall temperature [K]
T_{Zf} : average plume temperature at elevation, Z_{fl} [K]
T_∞ : ambient temperature [K]
t : time [sec]
v : vertical upward speed at height, Z_{fl} [m/s]
Z_{fl} : mean flame height [m]

* Frontier Technology Innovation Center, Chung-Ang University, 221 Huksuk-Dong, Dongjak-Ku, Seoul 156-756, Korea

Greek symbols

ε_w : wall emissivity
κ_i : absorption coefficient for the i-th gray gas
ρ_∞ : density of ambient gas [kg/m^3]
$\triangle \tau_i$: cell volume [m^3]
Ω, Ω' : scattering and incoming/outgoing direction

1. Introduction

In recent years, the atrium building has become commonplace. Other large open spaces include enclosed shopping malls, arcades, sports arenas, exhibition halls and airplane hangers. The smoke generated from fires in these spaces may cause people to panic and interfere with evacuation. Not only does the smoke generated from modern synthetic materials lead to disorientation and death of the occupants, but also large quantities of smoke become an obstacle to fire extinction. Therefore fire safety is an important issue to be considered by architects and engineers when they design the fire protection systems such as sprinklers and smoke control systems etc. However, there are few design guides with strong scientific backgrounds suitable for use by the construction industry.

The ability of sprinklers to suppress fires in spaces with ceilings higher than 11 to 15 m is limited.[1,2] Because the temperature of smoke decrease as it rises (due to entrainment of ambient air), the smoke may not be hot enough to activate sprinklers mounted under the ceiling of an atrium. Even if such sprinklers activate, the delay can allow fire growth to an extent beyond the suppression ability of ordinary sprinklers. Thus architects and engineers have to consider the smoke movement and temperature in atrium spaces. Many of the space characteristics of an atrium differ from traditional buildings. For example, if a fire occurs in the atrium, flame and smoke will spread vertically rather than horizontally to those parts of the building surrounding the atrium. The fire products are driven upwards within the interior of the atrium due to buoyancy force. It is difficult to control smoke movement in such a case with the conventional ventilation designs available.[3] Some studies have been done concerning prediction of smoke movement and temperature in atrium spaces.[4-6] Also, as the smoke movement is effected by a large number of inter-dependant processes including the stack effect and wind pressure, it is difficult and expensive to perform experimental studies with full-scale models. The alternative is to use computer simulation methods to determine the important physical parameters. Computer models are mathematical solutions implemented and displayed on computers. Zone model is a type of computer fire model that approximates the fire conditions in a room as two uniform layers with a source. This approach gives relatively coarse output for the building or room fire. A single temperature is computed for each zone as the fire develops in time. Another form of fire model is called a field model, ultimately yielding predictions for temperature and other variables at each point and for each time. Field model can be seen that the computation appears very realistic, Also it displays contours of constant temperatures at an instant in time that are colored in accordance with a real fire plume. The results are very impressive.

This study uses a self-developed SMEP field model[7] to the simulation of the smoke filling process in the two types of atrium spaces. The SMEP using PISO algorithm solves conservation equations for mass, momentum, energy and species, together with those for the modified $k-\varepsilon$ turbulence model with buoyancy production term. Also it solves the radiation equation using the discrete ordinates method. Compressibility is assumed and the perfect gas law is used. The SMEP are able to predict hot

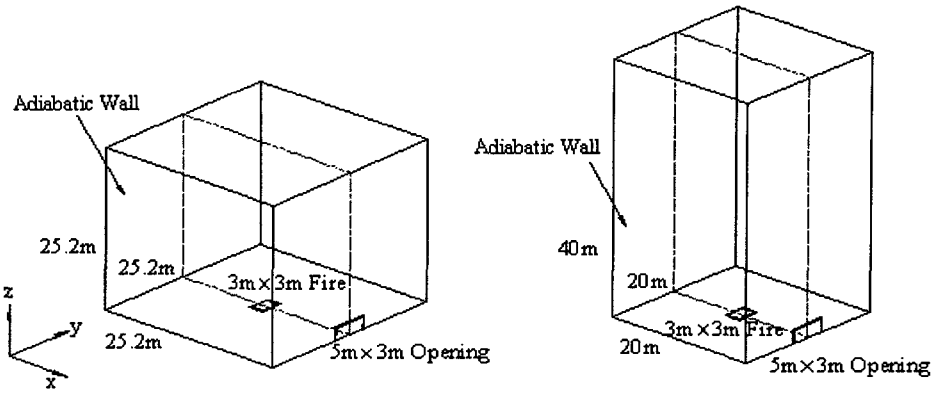

(a) Type 1 atrium (b) Type 2 atrium

Fig. 1 Geometry of the atrium halls.

smoke temperature and smoke layer clear height which are most important in fire safety considerations for atrium fires and offer data on required safe egress time. For atrium with ceiling glass the consideration of the ceiling heat flux by solar heat may be necessary in order to produce more realistic results. Also, this research compares the results with the zone model and SMEP field model. The zone models used are the CFAST developed at the Building and Fire Research Laboratory, NIST, U.S.A. and the NBTC one-room of FIRECALC developed at CSIRO, Australia. It is hoped to offer engineers and architects essential data for smoke movement in atrium fires.

2. Physical problem

In the simulation, two atrium buildings of same volume, 16,000 m^3, classified as type 1 and 2, are considered. Type 1 is of length 25.2 m, width 25.2 m and height 25.2 m; and type 2 is of length 20 m, width 20 m and height 40 m. The configurations and dimensions of two atrium spaces are shown in Fig. 1. In each case, there is a five meter wide by three meter high opening on the ground floor. A 3 m×3 m source is *located at the center of the floor. The heat* release rate of the fire, Q (in W), is increased as the square of time t (in s) and described by a fast mode of t^2 fire in the simulation as:

$$Q = 47t^2 \tag{1}$$

The fire was then kept at 1.5 MW after 178.6 s as shown in Fig. 2. For atrium the flow induced by this fire source is turbulent because the inertial force due to the density difference between the hot smoke and the ambient air is much greater than the viscous force. In this simulation, the modified $k-\varepsilon$ turbulence model with buoyancy term was used. The intensity of solar radiation passing into the ceiling glass during winter relative to summer is high. By considering the transmission and angle of in-

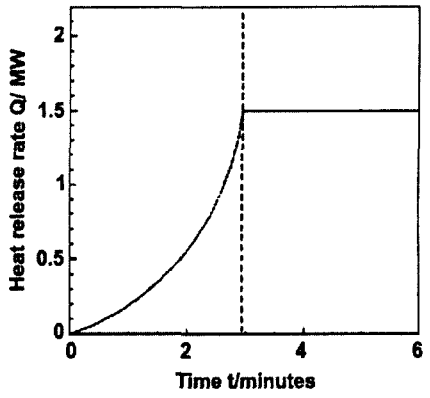

Fig. 2 Heat release rate used for the fire simulation.

cidence into a building through ceiling glass at noon of the winter a constant ceiling heat flux of 620 W/m^2 was used.

3. Mathematical models

3.1 Flow field model

The flow is described by the three-dimensional, Favre-averaged equations of transport for mass, momentum, gas species concentration and internal energy. Turbulence is modeled using the modified $k-\varepsilon$ equation model which were included to allow for the production of turbulence due to buoyancy and the effect of thermal stratification of the turbulence dissipation rate. We consider a thermally expandable ideal gas driven by a prescribed heat source. The equations of motion governing the fluid flow are written in a form suitable for low Mach number applications.

Sometimes, this form of the equations is referred to as weakly compressible. The most important feature of these equations is that in the energy equation the spatially and temporally varying pressure is replaced by an average pressure which depends only on time. Finite volume method and PISO algorithm are then employed for solving the linked set for velocity and pressure equations. The mathematical derivation are reported elsewhere[8,9] and will not be repeated here.

3.2 Radiation model

Radiant energy lost by the plume increases significantly temperature of the surrounding surfaces and modifies temperature and heat exchanges in the room. Radiation is produced by hot heteronuclear gas molecules and by soot particles. Soot production mechanisms are difficult to describe and depend on fuel nature and combustion conditions. We don't take account for their effects in the radiation model.

The S-N discrete ordinates method replaces the radiative transfer equation with a set of equations for a finite number of M ordinate directions.[10] To calculate the radiation equation in three-dimensional space, the 8 sweep directions are considered. The weighted diamond difference scheme is used in this study to relate the intensities in the control volume.[11] The total emissivity is equal to the absorption coefficient for a gray gas[12] and evaluated from the weighted sum of gray gases model (WSGGM) proposed by Schmidt et al.[13]

$$\varepsilon = \sum_{i=0}^{I} a_{\varepsilon,i}(T)[1-\exp(-\kappa_i ps)] \qquad (2)$$

where $a_{\varepsilon,i}$ which depend on the gas temperature T denote the emissivity weighting factors for the i-th gray gas. The bracketed quantity is the i-th gray gas emissivity with absorption coefficient, κ_i, and pressure-path length product, ps. For a gas mixture ps is the sum of the partial pressures of the absorbing gases. In the present analysis, three component gray gases are considered to represent the emissivity of the mixture (carbon dioxide, water vapor, and air). The expressions for the coefficients of the WSGGM are taken from the work of Schmidt et al.[13]

4. Numerical method

In SMEP field model, the difference schemes for discretizing the time term and the convection term into linear form used the Euler implicit scheme and the hybrid scheme, respectively.[14] The fire environment due to the same fire, of heat release rate given by equation (1), in the two atria was simulated using the field model. The two atrium halls were divided into $31\times23\times24$ and $31\times21\times27$ computing cells along the x, y and z (vertical direction) directions of a Cartesian co-ordinate system for the type 1

and 2 spaces, respectively. Within each time step, convergence was assumed if either the maximum number of iterations (100) was reached or the mass source residual fell to 1×10^{-3}. The time step used was 0.25 s and simulation was performed up to five minutes as this was considered sufficient time for people to evacuate the atrium safely. With regard to computing time, the SMEP using PISO algorithm was executed on a Pentium III 600 PC and the computing time required was less than five hours.

From the predicted air flow pattern and temperature fields, the smoke layer clear height is obtained by inspecting the positions where there are 1 percent of smoke concentration. The hot layer temperature is then taken to be the average value over all at the control cells in the smoke layer with each cell having a volume $\triangle\tau_i$ and temperature T_i:[6]

$$T_{av}=\frac{\sum_{\text{cells in the smoke layer}} T_i\triangle\tau_i}{\sum_{\text{cells in the smoke layer}}\triangle\tau_i} \tag{3}$$

4.1 Boundary and initial condition

The initial temperature and pressure were assumed to be 293 K and 101,325 Pa. Adiabatic wall boundary was assumed on the all of the side walls except the opening door and ceiling wall with heat flux by solar heat. A fixed pressure boundary condition was used on all external boundaries. Also the wall functions were used to bridge the near wall region. The wall boundary conditions to analysis the radiative heat transfer are all gray and diffusely reflecting, and they may also be sources for thermal radiation. The wall intensities are written as

$$I_w(x,y,z,\Omega)=\varepsilon_w T_w^4(x,y,z)+\frac{1-\varepsilon_w}{\pi}\int_{\Omega'\cdot\vec{n}<0}|\Omega'\cdot\vec{n}|I_w(x,y,z,\Omega')d\Omega' \tag{4}$$

$$\text{for}\quad \vec{n}\cdot\Omega>0$$

Where $\vec{n}$ is the inward normal unit vector to the boundary wall and ε_w is the wall emissivity.

4.2. Plume model and inlet condition

The flame height depends on the fire geometry, the ambient conditions, the heat of combustion and the stoichiometric ratio. A relationship[15] for flame height that can be used for many fuels is

$$Z_{fl}=0.235\dot{Q}^{2/5}-1.02D_f \tag{5}$$

Where Z_{fl} is the mean flame height, in meters, $\dot{Q}$ is the heat release rate of the fire, in kW and D_f is the diameter of fire, in meters.

The virtual origin of the plume,[16] $\triangle Z_f$ (m), is

$$\triangle Z_f=1.02D_f-0.083\dot{Q}^{2/5} \tag{6}$$

The virtual origin can be above the top of the fuel or below the fuel. The sign convention is: for the virtual origin above the top of the fuel $\triangle Z_f$ is negative, and for the virtual origin below the top of the fuel $\triangle Z_f$ is positive.

The mass flow, $\dot{m}$ (kg/s), of an axisymmetric plume at height Z_{fl}[17] is

$$\dot{m}=0.07\dot{Q}_c^{1/3}(Z_{fl}+\triangle Z_f)^{5/3}\times[1+0.026\dot{Q}_c^{2/3}(Z_{fl}+\triangle Z_f)^{-5/3}] \tag{7}$$

where $\dot{Q}_c$ is the convective heat release rate of fire, in kW. Because Smoke was defined to include the air that is entrained with the products of combustion, all of the mass flow in the plume is defined as being smoke. It follows that equation (6) can be thought of as an equation for the production of smoke from a fire. The convective of the heat release rate, $\dot{Q}_c$,

can be $\dot{Q}_c = \xi \dot{Q}$. Where ξ is the convective fraction of heat release. The convective fraction depends on the heat conduction through the fuel and the radiative heat transfer of the flames, but a value of 0.7 is often used for ξ.

The average temperature of the plume can be obtained from a first law of thermodynamics analysis of the plume. For the steady plume the work is zero, and the changes in kinetic and potential energy are negligible. The first law leads to an equation for the plume temperature:

$$T_{zf} = T_\infty + \frac{\dot{Q}_c}{\dot{m} C_p} \tag{8}$$

where T_{zf} is the average plume temperature at elevation Z_{fl}, in K, T_∞ is the ambient temperature, in K and C_p is the specific heat of plume gases, in kJ/kgK.

Fire plumes consist primarily of air mixed with the products of combustion, and the specific heat of plume gases is generally taken to be the same as air. The density of air and plume gases is calculated from the perfect gas law. The absolute pressure is taken to be standard atmospheric pressure of 101,325 Pa, and the gas constant is taken to be that of air which is 287 J/kgK.

The vertical upward speed v at height Z_{fl} above a fire for thermal plumes in free spaces can be expressed as

$$v = \frac{\dot{m}}{A \rho_\infty} \tag{9}$$

where v is the vertical upward speed of plume at height Z_{fl}, in m/s, A is the fire source area and ρ_∞ is the density of ambient gas. The inlet boundary conditions of fire source can be specified using the temperature T_{zf} and velocity v obtained from the above equations.

5. Numerical results and discussions

In the present study, the smoke filling process for the two types of atrium spaces were simulated using the two types of deterministic fire model: zone models and field model. The zone models used are the CFAST model developed at the NIST, USA and the NBTC 1-room model of FIRECALC developed at CSIRO, Australia. The field model is a self-developed SMEP field model based on computational fluid

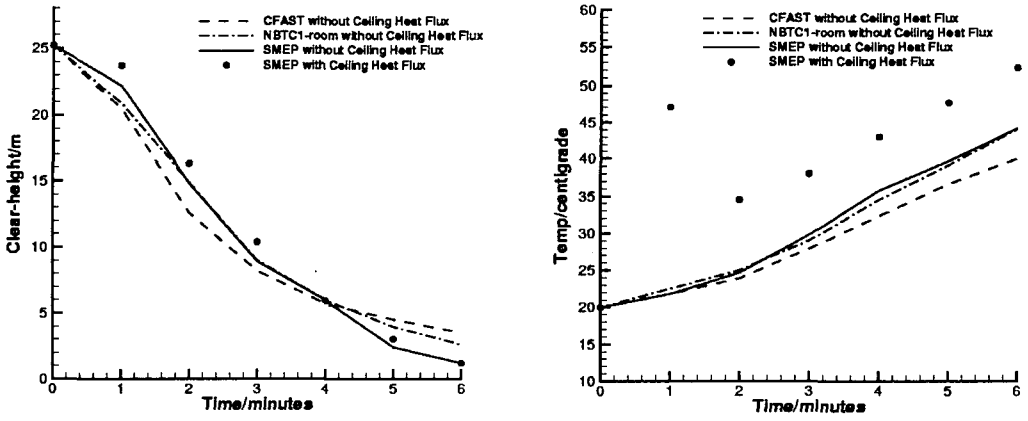

(a) Clear height (b) Average temperature

Fig. 3 Smoke layer clear height (a) and average temperature (b) in the type 1 atrium.

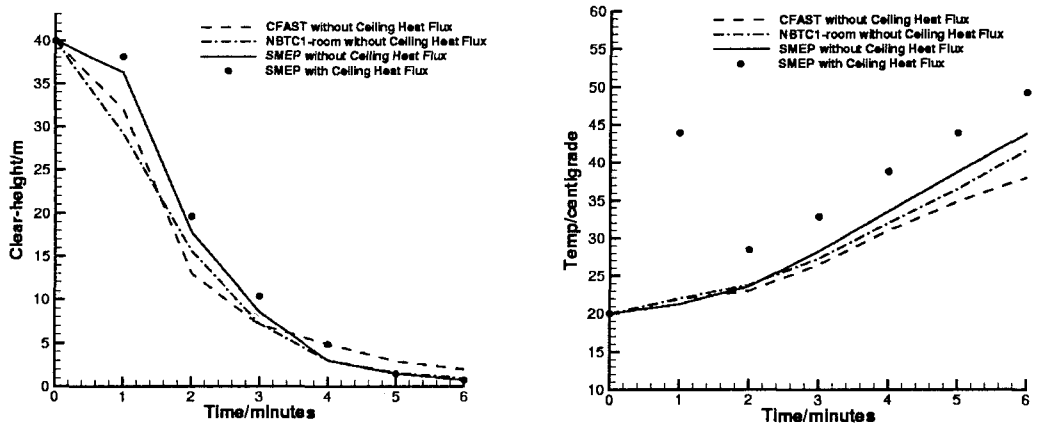

(a) Clear height (b) Average temperature

Fig. 4 Smoke layer clear height (a) and average temperature (b) in the type 2 atrium.

dynamics theories. Also, this paper describes the smoke movement and temperature distribution of SMEP code to the simulation of fire induced flows in the two types of atrium space containing a ceiling heat flux because the consideration of the ceiling heat flux by solar heat in atrium with ceiling glass is necessary in order to produce more realistic results.

The smoke layer clear heights and average temperatures of the simulated type 1 and type 2 atrium are shown in Figs. 3~4. For without ceiling heat flux, the results predicted by the two approaches are very similar. Thus, the SMEP field model is suitable for studying the smoke filling process in a large atrium space. In the type 1 atrium (Fig. 3(a)) and the type 2 atrium (Fig. 4(a)), the smoke layer clear heights predicted by the zone models and the SMEP without ceiling heat flux and with ceiling heat flux have very similar trends. On the other hand, the smoke layer average temperatures predicted by the zone models and the SMEP without ceiling heat flux and with ceiling heat flux in Fig. 3(b) and Fig. 4(b) deviated quite a lot. For example, a difference of about 24℃ in the early stage of a fire was found between the temperature predicted by the SMEP without ceiling heat flux and with ceiling heat flux. This seems to come from the thin hot layers formed by ceiling jet and the heat transfer from the ceiling glass by ceiling heat flux. However, the results of the smoke average temperature after 1 minute increase linearly in proportion to a difference of about 8℃ and 5℃, respectively. The results show that the smoke layer clear heights that are important in fire safety were not as sensitive as the smoke layer temperature to the nature of ceiling heat flux condition.

Fig. 5 and Fig. 6 show velocity vectors at 60 s and 180 s in the type 1 atrium after starting the fire. Like all the other cases of fire simulation, air was entrained from bottom of the plume as shown in these figures. Also, Fig. 5 and Fig. 6 show re-circulation regions in the surroundings of smoke plume and complex phenomena for the SMEP with ceiling heat flux. These phenomena seem to come from the velocity induced by the temperature difference between hot ceiling and surrounding gas. The ceiling heat flux condition shows relatively small re-circulation region in the surroundings of smoke plume. This seems to come from the accumulation of smoke induced the reduction of buoyancy force by ceiling heat flux.

Fig. 7 and Fig. 8 are the smoke temperature and the smoke concentration contours at 60 s. Because of the elevated temperature, buoyancy

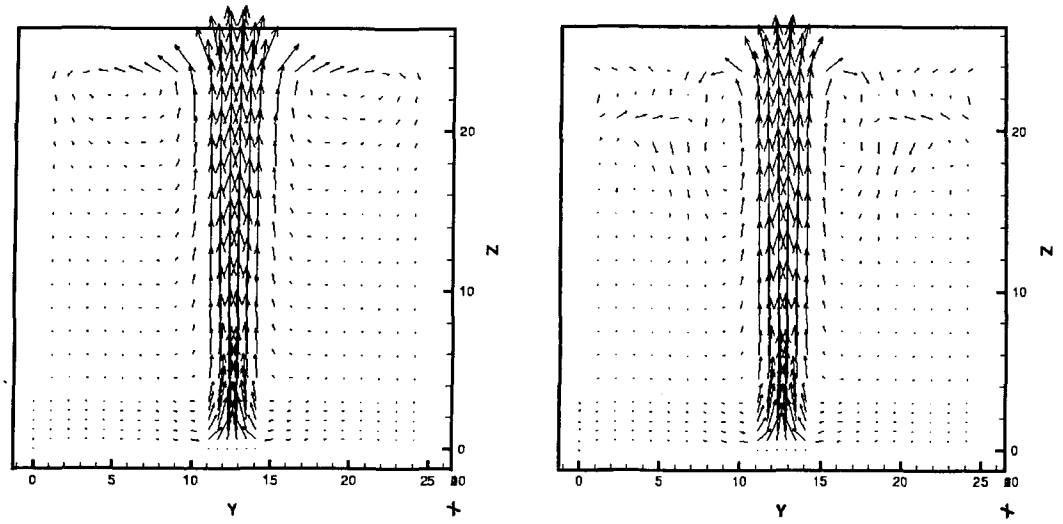

(a) Without ceiling heat flux (b) With ceiling heat flux

Fig. 5 Velocity vectors for type 1 atrium at 60 s.

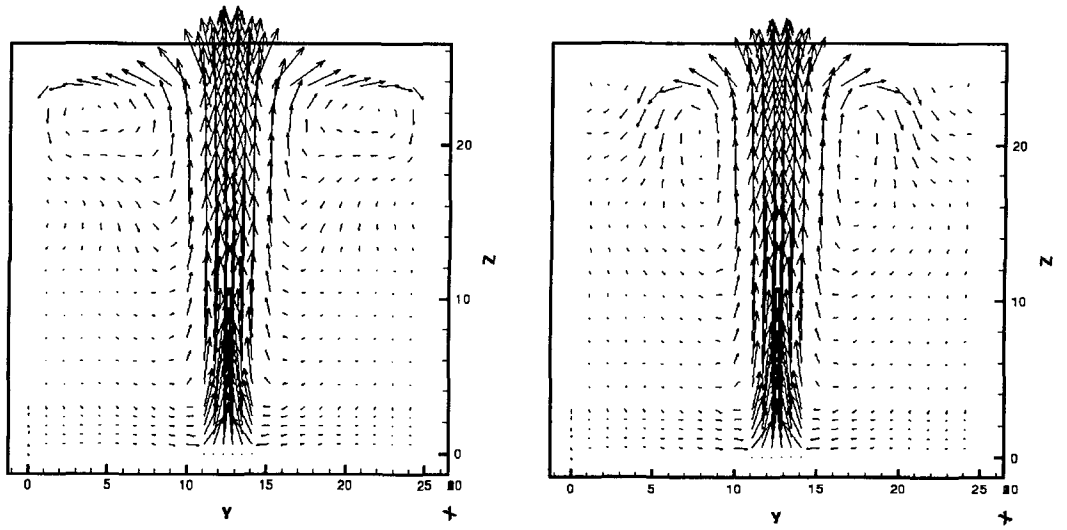

(a) Without ceiling heat flux (b) With ceiling heat flux

Fig. 6 Velocity vectors for type 1 atrium at 180 s.

forces drive gases upwards from the fire area towards the ceiling. In this way a plume is formed above the fire and relatively quiescent and cool gases at its periphery are laterally entrained and mixed with the plume gases. As a result of this entrainment the total mass flow in the plume continuously increases.

Fig. 9 and Fig. 10 show smoke temperature contours at 180 s. As depicted in Fig. 7 to Fig. 10, when the hot plume gases impinge on the ceiling, they spread across it forming a relatively thin radial jet and move outward under the ceiling surface. The hot gases transfer energy by convection and are retarded by fric-

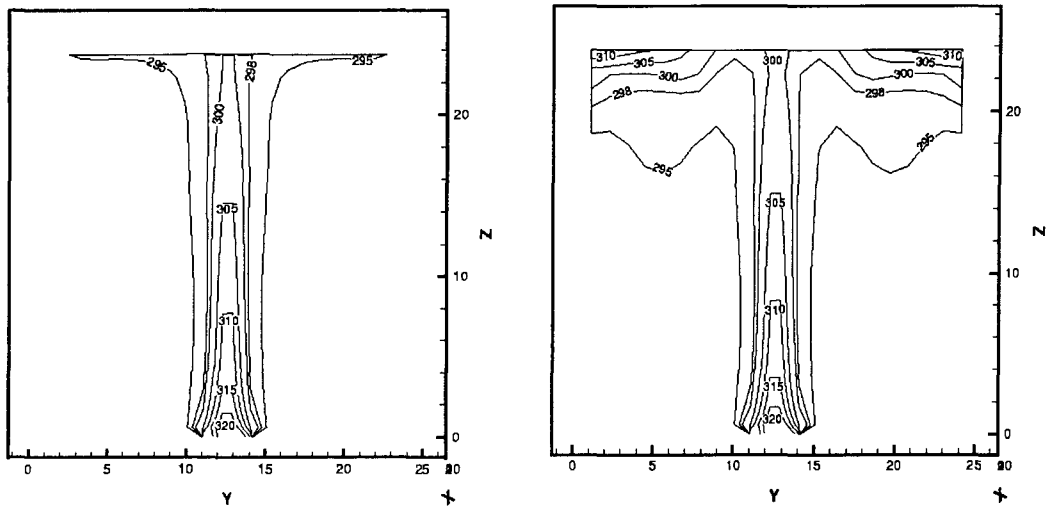

(a) Without ceiling heat flux (b) With ceiling heat flux

Fig. 7 Temperature contours for type 1 atrium at 60 s (All in K).

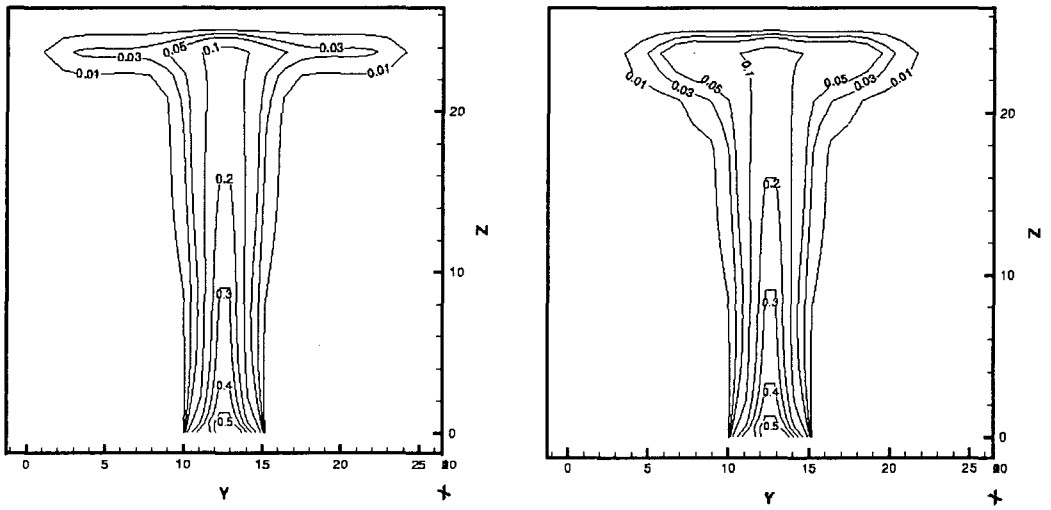

(a) Without ceiling heat flux (b) With ceiling heat flux

Fig. 8 Gas concentration contours for type 1 atrium at 60 s (All in ×100%).

tional forces from the ceiling surface above, and by turbulent momentum transfer to the entrained air from below. As a result of all this flow and heat transfer, the ceiling jet continuously decreases in temperature, smoke concentration and velocity; and increase in thickness with increasing radius. Because of the wall confining effect, the hot gases moved along the edge between the ceiling and the wall. The SMEP with ceiling heat flux has a high smoke temperature in near ceiling and forms a relatively thick radial jet. Also, because a low density induced by a high temperature near the ceiling decreases the buoyancy force and a low buoyancy and frictional force interfere with formation of downward wall

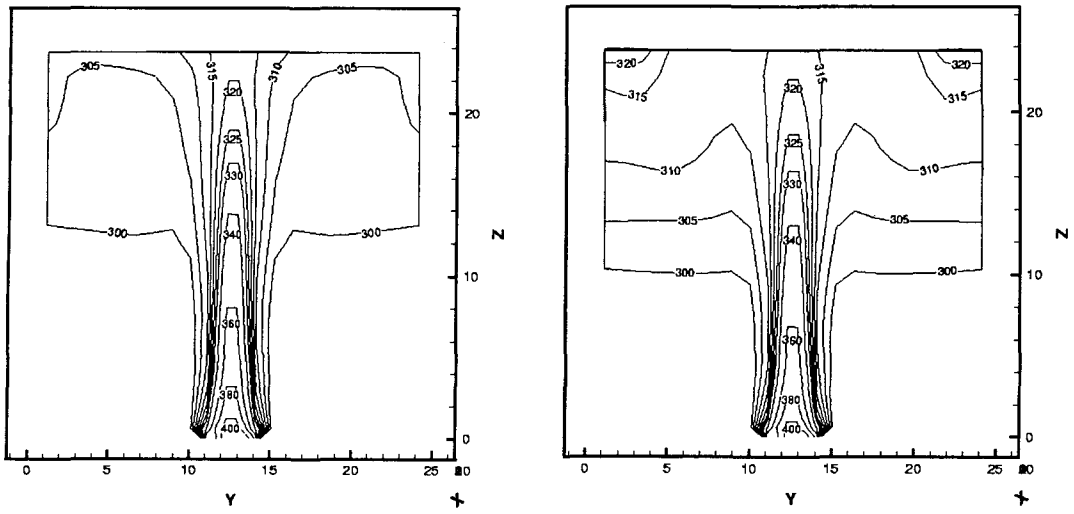

(a) Without ceiling heat flux (b) With ceiling heat flux

Fig. 9 Temperature contours for type 1 atrium at 180 s (All in K).

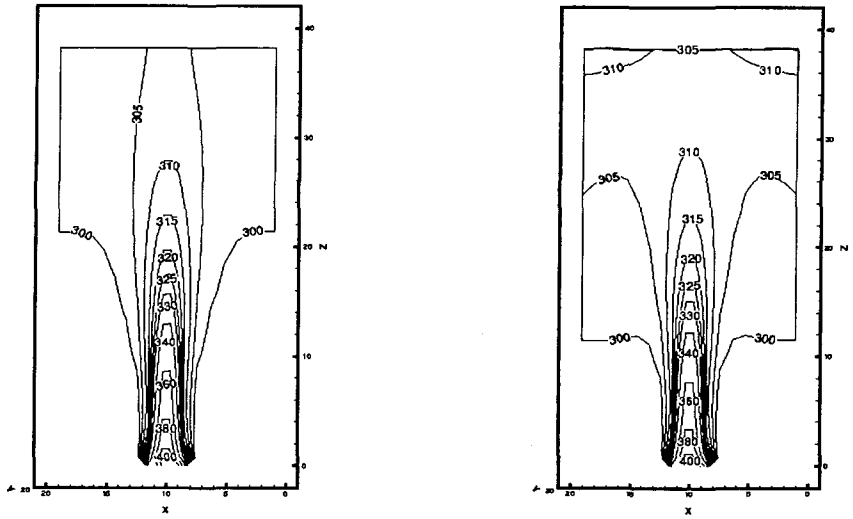

(a) Without ceiling heat flux (b) With ceiling heat flux

Fig. 10 Temperature contours for type 2 atrium at 180 s (All in K).

jet the accumulation phenomenon of higher temperature than the surrounding temperature appears in the corner between the ceiling and the side wall. This phenomenon causes a high smoke temperature near the ceiling. However, this ceiling heat flux condition has no effect on the smoke movement such as the smoke layer clear height as shown in Fig. 3(a) and Fig. 4(a).

Fig. 11 and Fig. 12 show the smoke average temperature below ceiling surface. For the early of the smoke formation near the ceiling after the start of a fire, a difference of a lot was found between the temperature predicted by the SMEP without ceiling heat flux and with ceiling heat flux but after about 3 minutes of the steady fire with constant heat release rate,

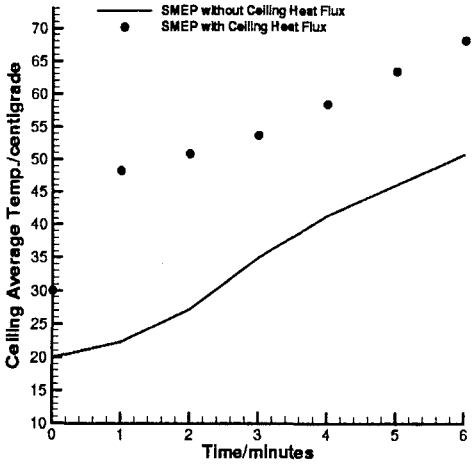

Fig. 11 Smoke average temperature in the near ceiling for type 1 atrium.

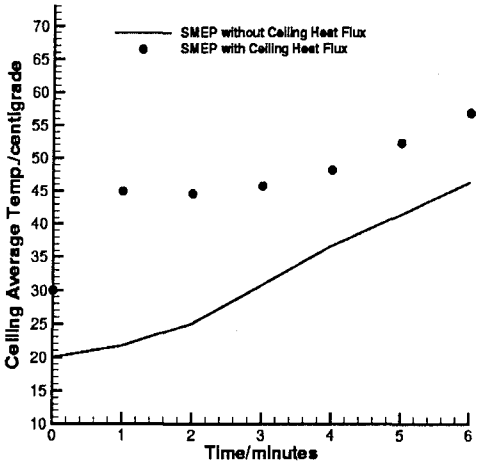

Fig. 12 Smoke average temperature in the near ceiling for type 2 atrium.

1.5 MW, the temperature near the ceiling increases linearly in proportion to time.

6. Conclusions

The results for the smoke layer temperatures and the smoke layer clear heights, predicted by CFAST, NBTC 1-room's zone model and SMEP field model are very similar. Thus, the SMEP model is proposed to substitute the zone model for predicting the smoke layer temperatures and the smoke layer clear heights because zone models assume that a stable and homogeneous smoke layer is formed, even in a large atrium spaces. Also it displays contours of constant temperatures and gas concentrations at an instant in time

For no consideration of ceiling heat flux, a large re-circulation regions along the wall between the ceiling and the side are caused by the effect of relatively thin ceiling jet and downward wall jet. On the other hand, the SMEP with ceiling heat flux has a high smoke temperature in near ceiling and forms a relatively thick radial jet. Because a low density induced by a high temperature near the ceiling decreases the buoyancy force and this low buoyancy force and frictional force interfere with formation of downward wall jet the accumulation phenomenon of higher temperature than the surrounding temperature appears in the corner between the ceiling and the side wall. Also, this ceiling heat flux condition shows relatively small re-circulation region in the surroundings of smoke plume. These phenomena cause a high smoke temperature near the ceiling. However, this ceiling heat flux condition by solar heat has no effect on the smoke movement such as the smoke layer clear heights that are important in fire safety.

The smoke layer clear height is about 3 m and 2 m respectively at 5 minutes, regardless of ceiling heat flux, for the two types of atrium after starting the fire. Therefore, the required safe egress time in the two types of atrium is about 5 minutes. In conclusion, the smoke layer clear heights that are important in evacuation activity except the early of a fire were not as sensitive as the smoke layer temperature to the nature of ceiling heat flux condition. Thus, a fire sensor in a large atrium space with ceiling glass has to consider these phenomena. Furthermore, additional quantitative validation of the model with experimental data must be performed. Work along all these lines is currently under way.

References

1. Degenkolb, J. G., 1975, Fire safety for Atrium Type Buildings, Building Standards, Vol. 44, No. 2, pp. 16-18.
2. Degenkolb, J. G., 1983, Atriums, Building Standards, Vol. 52, No. 1, pp. 7-14.
3. Kim, W. J., Yang, S. H. and Choi, K. R., 1993, The Experimental Study of Fire Properties in Atrium Space of High-rise Buildings, Journal of Korea Institute of Fire Science & Engineering, Vol. 7, No. 2, pp. 13-23.
4. Notarianni, K. A. and Davis, W. D., 1993, The Use of Computer Models to Predict Temperature and Smoke Movement in High Bay Spaces, National Institute of Standards and Technology, NISTIR 5304.
5. Chow, W. K. and Wong, W. K., 1993, On the Simulation of Atrium Fire Environment Hong Kong using Zone Model, Journal of Fire Science, Vol. 11, pp. 3-51.
6. Chow, W. K., 1995, A Comparison of the Use of Fire Zone and Field Models for Simulating Atrium Smoke-filling Process, Fire Safety Journal., Vol. 25, pp. 337-353.
7. Jeong, J. Y., Ryou, H. S. and Kim, S. C., 1999, A Numerical Study of Smoke Movement for the Three Types of Atrium Fires using PISO Algorithm, Journal of Korea Institute of Fire Science & Engineering, Vol. 13, No. 1, pp. 21-30.
8. Peric, M., 1985, A Finite Volume Method for the Prediction of Three Dimensional Fluid Flow in Complex Ducts, Ph.D., Imperial College.
9. Issa, R. I., 1985, Solution of the Implict Discretised Fluid Flow Equations by Operator-Spliting, Journal of Computational Physics, Vol. 62, No. 1, pp. 40-65.
10. Chandrasekhar, S., 1960, Radiative Transfer, Dover, New York, pp. 149-150.
11. Kim, T. K. and Lee, H. O., 1988, Effect of anisotropic scattering on radiative heat transfer in two-dimensional rectangular enclosures, Int. J. of Heat Mass Transfer. Vol. 31, No. 8, pp. 1711-1721.
12. Modest, M. F., 1991, The weighted sum of gray gases model for arbitrary solution methods in radiative transfer. J. of Heat Transfer, Vol. 113, pp. 650-656.
13. Schmidt, T. F., Shen, Z. F. and Friedman, J. N., 1982, Evaluation of coefficients for the weighted sum of gray gas model, J. of Heat Transfer, Vol. 104, pp. 602-608.
14. Patankar, S. V., 1980, Numerical Heat Transfer and Fluid Flow, McGraw Hill-Washington, D.C., pp. 25-40.
15. Heskestad, G., 1988, Fire Plumes, SFPE Handbook of Fire Protection Engineering, Society of Fire Protection Engineers, Boston, MA.
16. Heskestad, G., 1983, Virtual Origins of Fire Plumes, Fire Safety Journal, Vol. 5, No. 2, pp. 109-114.
17. Heskestad, G., 1984, Engineering Relations for Fire Plumes, Fire Safety Journal, Vol. 7, No. 1, pp. 25-32.